Journal of Building Engineering 47 (2022) 103861

Contents lists available at ScienceDirect

Journal of Building Engineering

journal homepage: www.elsevier.com/locate/jobe

Shear behaviour of reinforced construction and demolition waste-based geopolymer concrete beams

Alper Aldemir [a,*], Saban Akduman [a], Oznur Kocaer [a], Rafet Aktepe [a], Mustafa Sahmaran [a], Gurkan Yildirim [a], Hanady Almahmood [b], Ashraf Ashour [c]

[a] Hacettepe University, Department of Civil Engineering, Ankara, Turkey
[b] Department of Civil Engineering, BD7 1DP, UK
[c] Bradford University, Department of Civil Engineering, BD7 1DP, UK

ARTICLE INFO

Keywords:
Construction and demolition waste
Reduced CO_2 emission
Recycled aggregate
Geopolymer
Shear-deficient flexural tests
Sustainable construction

ABSTRACT

Geopolymer concrete (GPC) is a promising candidate to replace conventional concrete (CC) as geopolymer concrete depends on alkali-activated binders instead of Portland cement. The elimination of cement from the mixture results in the reduction of the greenhouse gas release. From the literature, it is known that the micro-scale characteristics of the geopolymer concrete are similar to its counterparts. However, the structural performance of geopolymer elements should be investigated in detail. Therefore, in this study, the deficiently reinforced beams' structural performance was compared by conducting bending tests to determine the shear behavior of new geopolymer concrete manufactured from entirely construction and demolition wastes (CDW). In these experiments, geopolymer concrete with recycled aggregates, geopolymer concrete with natural aggregates, concrete with recycled aggregates, and concrete with natural aggregates were used in order to study the possibility of reaching fully-recycled construction materials. Three shear span-to-effective depth ratio were used to examine the different failure modes. The mechanical performances of geopolymer concretes were assessed by using load-deflection/moment-curvature curves, and crack propagations. Test results revealed that geopolymer concrete beams exhibited similar performance to the concrete beams of the same grade. Besides, the insertion of recycled aggregates caused a shift in the failure mechanism from flexure-dominated to shear-dominated, especially in specimens with larger a/d ratios. Finally, the capacity prediction performance of current codes, i.e., TS500 and ACI318, were also examined, and the calculations resulted that the current code equations had a percentage error of approximately 55% on average, although TS500 equations performed slightly better.

1. Introduction

Concrete forms the backbone of the construction industry all over the world. However, during concrete production, significant amounts of naturally available raw materials are consumed, releasing greenhouse gases into the atmosphere that triggers one of the major issues faced today; global warming. In general, the production of 1 ton of Portland cement (PC) requires around 1.5 tons of raw

* Corresponding author.
E-mail addresses: alperaldemir@hacettepe.edu.tr (A. Aldemir), akduman501@gmail.com (S. Akduman), oznurkocaer@hacettepe.edu.tr (O. Kocaer), rafet.aktepe@hacettepe.edu.tr (R. Aktepe), sahmaran@hacettepe.edu.tr (M. Sahmaran), gurkanyildirim@hacettepe.edu.tr (G. Yildirim), h.a.a.a.almahmood@gmail.com (H. Almahmood), A.F.Ashour@bradford.ac.uk (A. Ashour).

https://doi.org/10.1016/j.jobe.2021.103861
Received 14 October 2021; Received in revised form 3 December 2021; Accepted 8 December 2021
Available online 10 December 2021
2352-7102/© 2021 Published by Elsevier Ltd.

materials, and as a result, 0.9 tons of CO_2 are emitted [1,2]. It should also be noted that manufacture of Portland cement generates vast amount of waste and increases greenhouse gases by about 7% [3]. Furthermore, Portland cement manufacturing process necessitates a significant amount of energy. As a result, it is clear that the immoderate usage of Portland cement is unmaintainable. As a consequence, the development of ecologically friendly and cost-effective construction materials should be prioritized globally. Besides, concrete production requires aggregates of different sizes whose production process is also highly energy-intensive and creates significant amounts of waste. In recent decade, growing awareness of sustainability and global warming issues have been swaying construction industry to search for a more environmental friendly alternative. As a result of the ever-increasing urban population and the continuously developing economies of countries in the world, the construction and demolition industry gained eye-catching popularity, despite being one of the world's largest solid waste contributor. These wastes, mainly destined for landfills and contain harmful compounds, might endanger the environment and the community's health if they are not properly managed. Therefore, handling this construction demolition waste (CDW) in an appropriate manner for the sake of environmental, social, and economic benefits is crucial [4,5].

Along with the environmental issues of cement production and aggregate quarrying, conventional concrete is not long-lasting. It tends to deteriorate under the influence of mechanical and environmental impacts, leading to structural demolition and creating significant amounts of waste concrete and masonry units. Thus, it is now a question of debate to find appropriate places for the disposed waste concrete [6]. To address this effectively, researchers have already started to look for new methods to recycle the construction demolition wastes. One way is to directly crush the waste concrete and obtain aggregates in different sizes. Although the process seems very simple, what to do with the resulting product is an object of interest. Recycled coarse aggregates are generally used in low-tech applications such as a base course in pavements and filling purposes with no structural capability [7].

Geopolymer concrete is promising to be a versatile alternative to conventional concrete as this construction material could limit the emission of CO_2 gases and help the reduction of construction demolition waste. It is common knowledge that cement-containing building materials have insufficient performance under tension and has limited ductility in the absence of reinforcements. In addition, the shear behavior of cement-based materials also exhibits a brittle failure, which should be prevented to achieve proper seismic designs. Instead of cement, geopolymer concrete is made with activated pozzolanic ingredients and aggregates [8]. In addition, carbon footprint of geopolymer-based concrete is 80–90% less than conventional concrete since it is produced mainly from industrial wastes like slag, recycled concrete, fly ash, recycled bricks, glass powder, etc. [9,10]. Nevertheless, the current literature on the structural use of geopolymer concrete is not matured [11–18]. For instance, Raj et al. [11] reported an investigation to analyze the behavior of geopolymer concrete joints, which was claimed to perform better when subjected to cyclic loading. In a study conducted by Ahmet et al. [12], the effects of glass fiber reinforced polymer (GRFP) bars on geopolymer beams were investigated. In addition, Wu et al. [13] subjected the geopolymer beams produced with slag to shear tests to examine the influence of transverse reinforcement on different characteristics like strength of concrete, ratio of longitudinal reinforcement, ratio of shear span/depth, and depth of the beam. They used ambient-temperature curing, contrary to the work conducted by Sumajouw et al. [14]. They concluded that slag-based geopolymer had similar behavior as far as the crack distribution and failure mode of specimens were compared. In short, all the researchers analyzed the properties of geopolymer concrete structural elements with slag/fly ash and never focused on the effect of the inclusion of waste materials. The influences of using the recycled aggregates and the exclusion of fly ash or slag from the geopolymer mixture on the shear strength of slag-based GC beams need to be further investigated. This investigation will help design engineers to reach a more environment-friendly constructional material. Tran et al. [15] investigated the shear behavior of ambient-cured geopolymer concrete beams reinforced with basalt fiber reinforced polymers. In their experiments, Tran et al. [15] would not include any stirrups and the geopolymer concrete shear performance was solely obtained. In addition, Akduman et al. [16] and Tran et al. [17] studied the flexural behavior of ambient cured geopolymer concrete beams reinforced with steel fibers. Farhan et al. [18] was obtained the behaviour of ambient cured steel fibre reinforced geopolymer concrete columns under axial and flexural loads. They tested sixteen circular geopolymer concrete column specimens of 150 mm diameter and 600 mm height. Three types of steel fibres (straight micro steel fibre, deformed macro steel fibre and hybrid steel fibre) were used in reinforcing the geopolymer concrete column specimens.

In this study, the structural performance of beam elements produced from new geopolymer concrete was determined. To this end, geopolymer beams were tested via four-point loading with a displacement-controlled protocol. The control variable in these tests was the base material (i.e., concrete). Four different base materials were utilized: i. Conventional concrete (C Specimens), ii. New geopolymer concrete (NGC Specimens), ii. Conventional concrete with recycled aggregate (C-R Specimens) and iv. New geopolymer concrete with recycled aggregate (NGC-R Specimens). The geopolymer beams were cured under ambient conditions until the day of the tests. 150 × 250 × 1100 mm (width × height × length) rectangular ½ scaled beam specimens were produced with deficient lateral reinforcement detailing (i.e., less amount of lateral reinforcement was placed than the code required in accordance with TEC2018 [19]). In each experiment, the load-midspan vertical displacement curves, moment-curvature curves, and detected pattern of crack were recorded. In addition, each specimen was tested for three different shear-span-to-depth ratios to investigate the effect of the a/d ratio on the failure modes. Therefore, the effect of the using of recycled aggregates on the shear performance of reinforced geopolymer beams with deficient lateral reinforcement detailing is also examined.

2. Details on fully recycled geopolymer concrete

2.1. CDW materials

The produced geopolymer concrete was aimed to be made from fully recycled construction demolition waste (CDW) material; therefore, masonry units (i.e., red clay brick (RCB), hollow brick (HB), and roof tile (RT)), concrete rubble (CRB) and waste glass (G) were gathered from a demolition site in Eskişehir, Turkey. These collected CDWs were subjected to sequential crushing and grinding

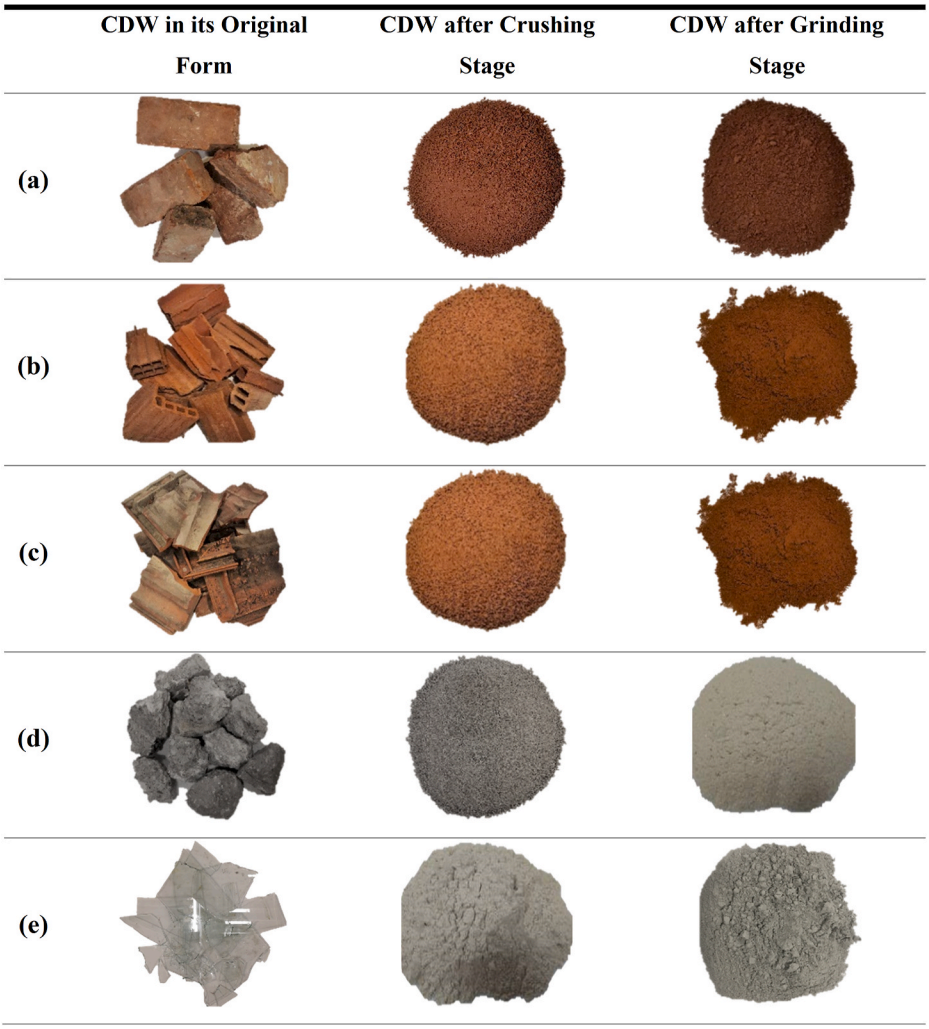

Fig. 1. Photographs of CDW-based materials: (a) Red clay brick, (b) Hollow brick, (c) Roof tile, (d) Concrete rubble and (e) Glass. (For interpretation of the references to colour in this figure legend, the reader is referred to the Web version of this article.)

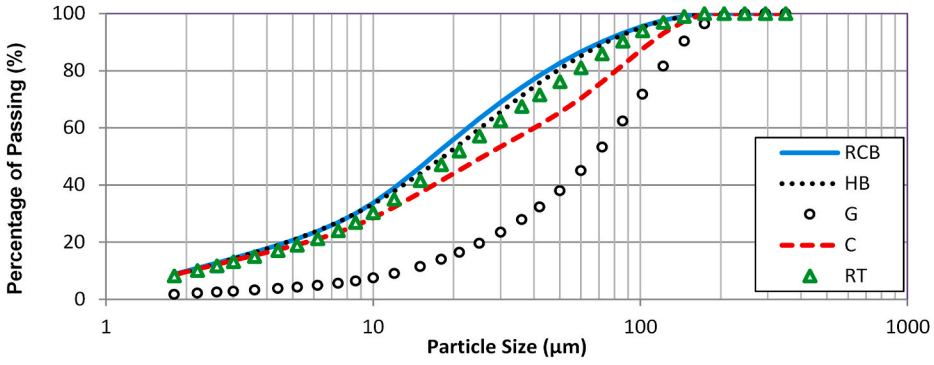

Fig. 2. Particle size distributions of different CDW materials.

procedures. The first step of this two-stage procedure is the preparation of CDW-based materials for the grinding process. To this end, at first, the CDWs (i.e., masonry units, concrete rubble, glass, etc.) were crushed with a laboratory scale jaw crusher to reduce the particle size. Then, these crushed CDWs were ground via laboratory scale ball-mill for approximately an hour. In Fig. 1, visuals of the CDW-based materials used in this study are presented before and after each procedure. At the end of this sequential crushing and

Table 1
Chemical compositions of CDWs.

Chemical composition, %	CDW-based precursor			
	Red clay brick (RCB)	Hollow brick (HB)	Roof tile (RT)	Glass (G)
Loss on ignition	2.18	1.99	2.11	0.29
SiO_2	53.4	61.6	54.0	73.4
Al_2O_3	20.5	17.3	15.9	1.27
Fe_2O_3	7.77	6.70	8.93	0.18
CaO	4.75	3.31	7.42	10.9
MgO	3.70	2.66	4.84	0.18
SO_3	1.16	0.38	0.68	0.10
Na_2O	1.53	1.61	1.41	12.8
K_2O	3.42	2.80	2.30	0.08

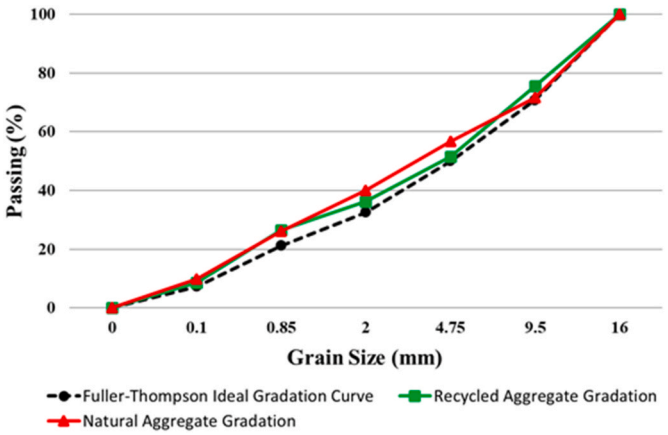

Fig. 3. The particle size distribution of the NAGs and RAGs.

Table 2
Properties of recycled and natural aggregates.

Size	Recycled Aggregates (RAG)		Natural Aggregates (NAG)	
	16.00–4.75 mm	<4.75 mm	16.00–4.75 mm	<4.75 mm
Dry Specific Gravity (g/cm^3)	2.23	1.86	2.68	2.64
SSD Specific Gravity (g/cm^3)	2.32	2.11	2.69	2.67
Apparent Specific Gravity (g/cm^3)	2.46	2.51	2.71	2.72
Water Absorption (%)	4.20	13.80	0.29	1.24
Loose Unit Weight (g/cm^3)	1.22	1.44	1.47	1.67
Dense Unit Weight (g/cm^3)	1.35	1.58	1.54	1.80

grinding process, the particle size distributions of each CDW were also obtained and are summarized in Fig. 2.

The chemical composition of the waste materials was also obtained by performing XRF analyses. The results are summarized in Table 1.

In this study, maximum particle size was 100 μm. It should be noted that, if fractions having $D_{50} < 15$ μm are utilized, substantial increases in the mechanical properties of geopolymers can be obtained [20,21]. However, the effort and duration at the grinding stage were not increased to reach finer particle fractions in this study as further grinding was more energy-intensive, which created a contradiction to achieve more sustainable construction material.

Recycled aggregates (RAG) are obtained from the crushing of concrete rubbles taken from the demolition sites and separating crushed particles by using sieves with various openings. Another type of aggregate used in mixtures is natural aggregates (NAG). In order to eliminate errors that may arise from the gradation difference of two different types of aggregates in the results of the experiment, the granulometry of NAG and RAG was manually approximated to the Fuller-Thompson ideal gradation curve. The size of the maximum aggregate (D_{max}) was chosen 16 mm. Particle size distributions of the NAGs and RAGs are given in Fig. 3.

Specifications of aggregates are another crucial parameter to design concrete and geopolymer mixes and all of these parameters affect resulting product. Properties of RAG and NAG that are used in the geopolymer and concrete mixtures are summarized in Table 2. While the specific gravity and unit weight of natural aggregates are higher than those of recycling aggregates, it can be seen that the water absorption property of recycling aggregates are considerably higher than natural aggregates. Moreover, the unit weight of the

Table 3
Proportions for completely CDW-based geopolymer concrete and conventional concrete mixtures.

Materials (kg/m^3)	NGC	NGC-R	C	C-R
Roof Tile	250	250	–	–
Red Clay Brick	200	200	–	–
Hollow Brick	150	150	–	–
Glass	100	100	–	–
Concrete Rubble	100	100	–	–
Portland Cement	–	–	316	316
Slag	150	150	–	–
Fly Ash	50	50	–	–
Calcium Hydroxide	50	50	–	–
Sodium Hydroxide	112	112	–	–
Sodium Silicate	224	224	–	–
NAG (Fine)	500	–	917	–
NAG (Coarse)	500	–	917	–
RAG (Fine)	–	500	–	917
RAG (Coarse)	–	500	–	917
Water	202.16	202.16	211	211
Water/Binder	0.35	0.35	0.67	0.67

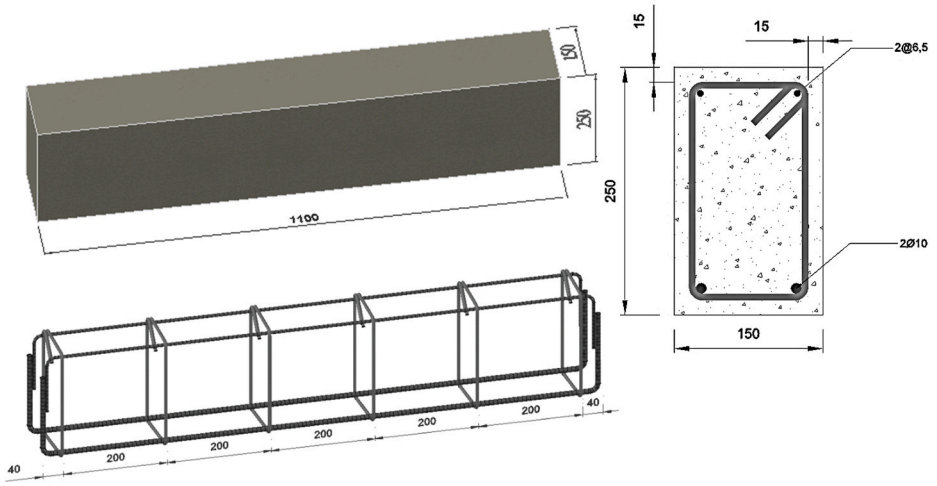

Fig. 4. Reinforcement details of the test specimens*
All dimensions are given in mm.

Table 4
Mechanical properties of test specimens.

Specimens	Average Concrete Compressive Strength (MPa)	Average Concrete Splitting Tensile Strength (MPa)
NGC Specimens	37.50 (2.83)*	2.56 (0.29)
NGC-R Specimens	36.60 (2.06)	2.37 (0.31)
C Specimens	34.10 (1.32)	2.45 (0.15)
C-R Specimens	35.20 (1.60)	2.21 (0.17)

*: Numbers in parentheses are standard deviations.

recycling aggregates increases as the grain size decreases.

2.2. Details on the new geopolymer concrete

There are mainly two steps in the preparation of geopolymer mixtures. In the first step, the liquified alkaline activator is prepared. In the second stage, this prepared liquified alkaline activator is mixed with the other ingredients: alkaline activators in powdered form (i.e., Calcium hydroxide and sodium silicate), ground CDWs, aggregates, and water. The preparation of the liquified alkaline activator is the dissolution of sodium hydroxide flakes in the water at a Na + concentration of 6.44, corresponding to a NaOH molarity of 8 M in the whole system. Then, this solution was allowed to cool down to room temperature for one day. From the preliminary mixtures, it experimented that the geopolymer concrete produced from only liquified alkaline activator resulted in setting times more than 6hrs and exhibited low mechanical properties. Therefore, other alkaline activators (i.e., calcium hydroxide and sodium silicate) were added

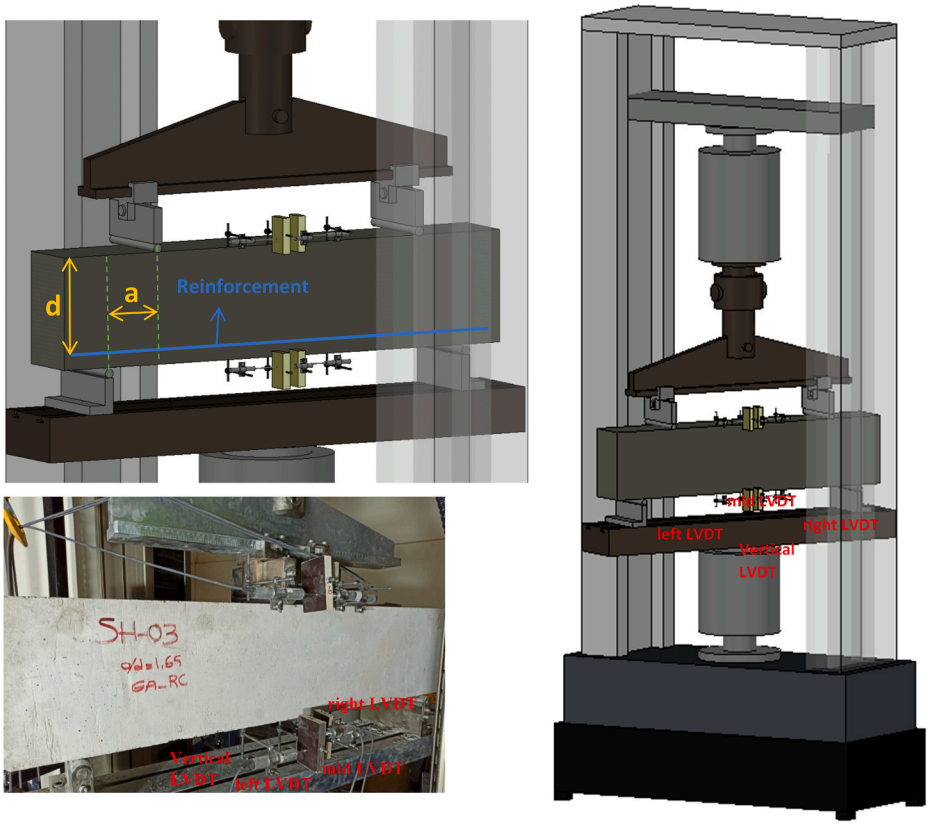

Fig. 5. Test setup and instrumentation.

Table 5
Test parameters.

Parameters		
F_u	Ultimate Force	
F_y	Yield Force	Calculated by considering the procedure of bilinearization in FEMA356 [46]
u_u	Ultimate Displacement	Displacement equal to the end of the experiment results or the %20 drop capacity
u_y	Yield Displacement	Yield displacement calculated by making use of the bilinearization procedure in FEMA356 [46]
$\mu_u = \frac{u_u}{u_y}$	Ductility	
Φ_u	Ultimate curvature	Curvature equal to the end of the experiment results or the %20 drop capacity
φ_y	Yield curvature	In FEMA356, yield curvature is calculated by utilizing the bilinearization technique
$\mu\varphi = \frac{\varphi_u}{\varphi_y}$	Curvature ductility	
E_t	Energy dissipation capacity	
$En = \frac{Et}{Fy \times \frac{uy}{2}}$	Normalized energy capacity	

to the mixture to decrease the setting time of the mix (i.e., less than 2hrs) and improve the mechanical properties significantly. Besides, the strength and the workability of the concrete mixture were enhanced by including slag and fly ash (other production wastes) into the mixture. These modifications on the geopolymer concrete enabled to be cured at ambient temperatures as combining different types of alkali activators and/or substitution with industrial by-products. The water to binder ratio was selected as 0.35 for all geopolymer mixtures. The details on the proportions of all the ingredients of geopolymer concrete are provided in Table 3. It should be noted that no further chemical additive was utilized to prevent any potential interactions with the alkali solution. Detailed information on the content of geopolymer concrete was given in recent studies [4,5].

In this study, four different mixtures with two different paste compositions (i.e., conventional concrete and geopolymer concrete) were prepared to examine the performance of new geopolymer concrete. To this end, the geopolymer concrete was produced by using natural aggregates (NGC Specimens) and recycled aggregates (NGC-R Specimens). Consequently, control specimens were also

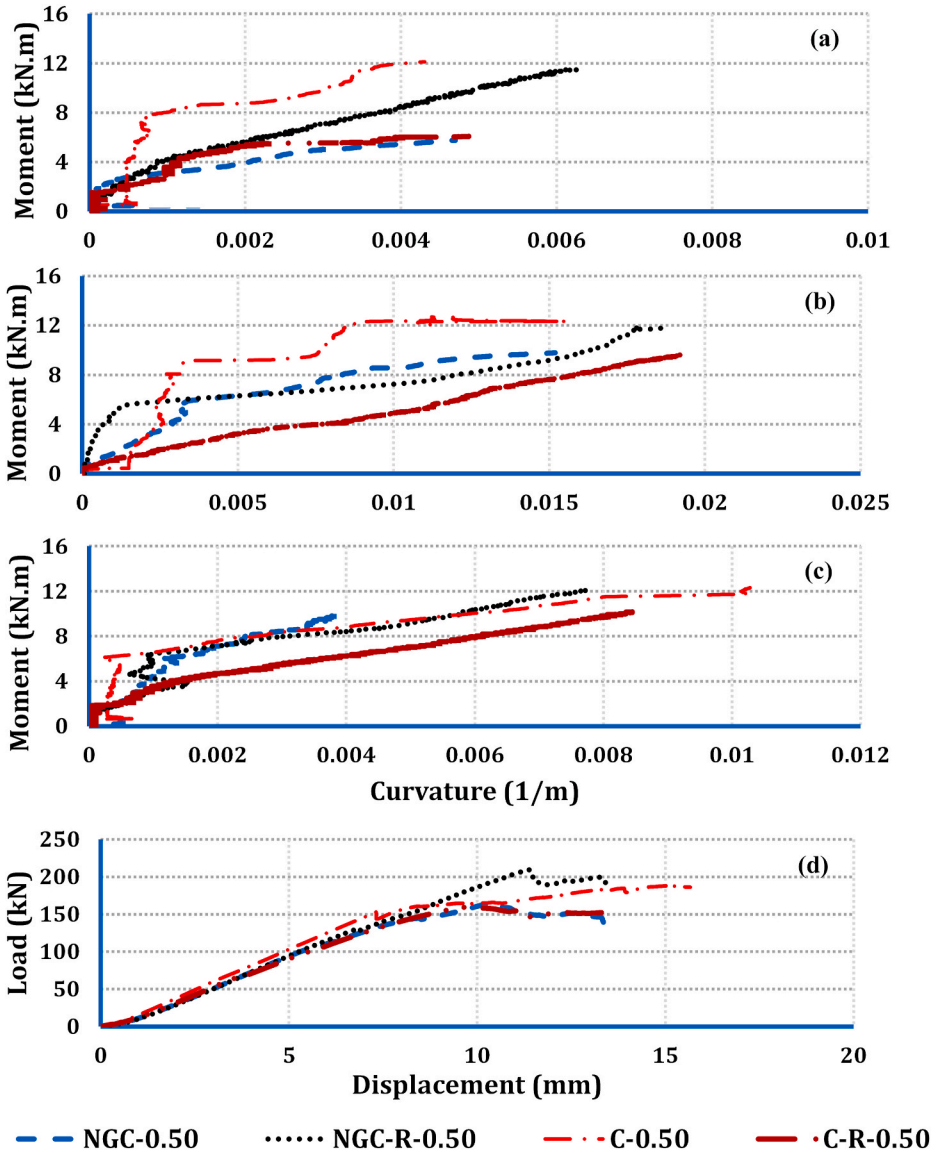

Fig. 6. M − ϕ Relationship for a/d = 0.50: (a) the M-ϕ curve of left LVDTs, (b) the M − ϕ curve of mid-LVDTs, (c)M-ϕ curve of right LVDTs, and (d) Total vertical load-midspan vertical displacement.

prepared from conventional concrete with natural aggregates (C Specimens) and recycled aggregates (C-R Specimens).

3. Details on test specimens and testing

The shear performance of the new geopolymer concrete was investigated in the current study. Therefore, three shear-span to effective depth (a/d) ratios (0.50, 1.00, and 1.65) were selected to investigate various possible failure modes. The geometrical properties and reinforcement details of the tested specimens were chosen from the first-story central-internal bay of a three-story prototype RC building designed in accordance with the current Turkish seismic code (TEC2018 [19]). The selected prototype beam had a 300 × 500 mm rectangular cross-section. The dimensions of the beam represent typical values in RC frames [22]. Specimens scale was chosen as ½ considering the limitations of the facilities. Such scaled specimens were used successfully in the past for the cyclic testing of frames by others [23–26]. Thus, the tested rectangular beam specimen had a width of 150 mm and a height of 250 mm (i.e., 150 × 250 mm beams). The decision on the stirrup spacing was made in comparison with the prototype beam member. The selected prototype beam had stirrups spaced at a 100-mm interval. This prototype beam was designed to be flexure-dominant. Therefore, the scaled test specimens were modified in order to shear-dominated behavior. To this end, the stirrup spacing was taken four times the prototype beam, which corresponds to a stirrup spacing of 200 mm. This manipulation was solely to have shear-dominated failure. In addition, fine and coarse aggregates have been used in the production of geopolymer concrete. The

Table 6
Test results summary.

Parameters	Shear span-to-depth ratio (a/d)											
	0.50				1.00				1.65			
	C	C-R	NGC	NGC-R	C	C-R	NGC	NGC-R	C	C-R	NGC	NGC-R
Ini. Stiff.	31,661	28,301	30,198	29,230	33,333	32,692	32,608	30,408	21,739	18,285	20754	18,867
F_y *(kN)*	187.06	155.26	156.39	198.96	168.10	165.31	170.78	162.47	106.59	91.35	91.89	94.79
F_u *(kN)*	195.24	159.94	164.18	206.32	190.03	191.49	192.4	190.4	110.82	94.93	103.89	98.63
M_y *(kN.m)*	10.62	9.31	9.38	11.94	21.01	20.66	21.35	20.31	20.79	17.81	17.92	19.26
M_u *(kN.m)*	11.71	9.60	9.85	12.38	23.75	23.94	24.05	23.80	21.61	18.51	20.26	19.04
u_y *(mm)*	10.50	8.50	8.55	11.50	8.91	10.21	10.18	9.56	9.11	9.21	9.25	9.15
u_u *(mm)*	15.18	13.78	13.89	13.86	13.18	16.47	19.05	15.34	30.57	14.41	35.05	14.51
φ_y *(1/m)*	0.0055	0.0198	0.0060	0.0031	0.017	0.020	0.021	0.019	0.035	0.031	0.052	0.035
φ_u *(1/m)*	0.0153	0.0198	0.0151	0.0181	0.076	0.096	0.103	0.092	0.206	0.181	0.231	0.175
μ_u	1.45	1.62	1.62	1.21	1.48	1.61	1.87	1.60	3.36	1.56	3.79	1.59
μ_φ	2.78	1.00	2.52	5.84	4.47	4.80	4.90	4.84	5.89	5.84	4.44	5.00
E_t *(kN.m)*	2.345	1.509	1.515	2.201	1.425	1.974	2.378	1.719	2.617	1.170	3.028	0.999
E_n	2.388	2.287	2.266	1.924	1.903	2.339	2.736	2.213	5.390	2.781	7.125	2.304

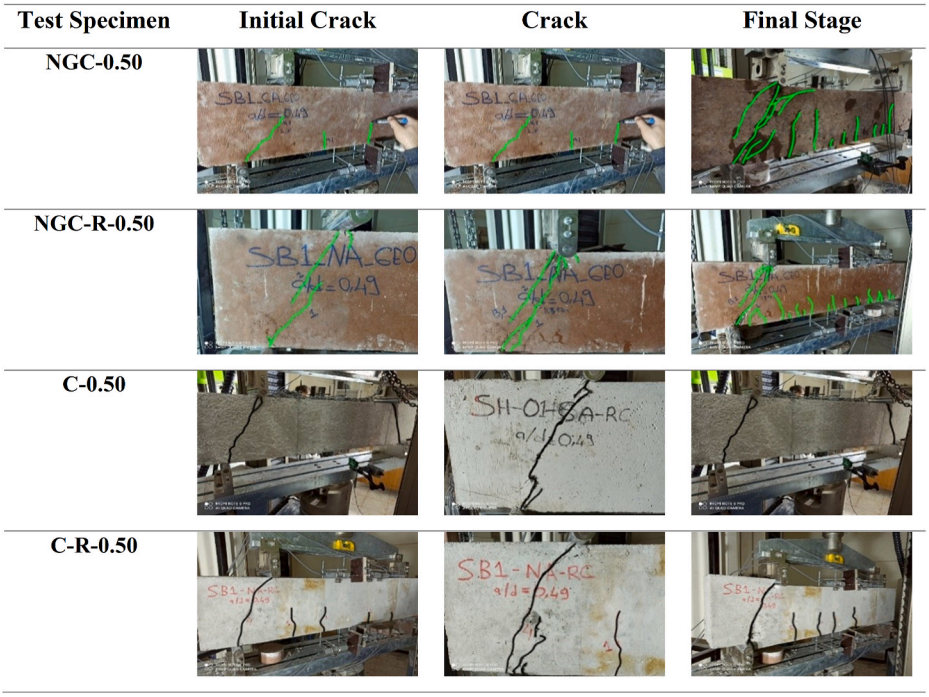

Fig. 7. Pattern of crack propagation of specimens (a/d = 0.50).

maximum aggregate size (MAS) was selected as 10 mm in order not to violate the laws of similitude [27–29] since the MAS of the prototype specimens was 16 mm. In other words, the scaling process was aimed to generate the same stress demands on both the prototype and the scaled specimens but the fracture energy of the prototype and scaled concrete mixtures should be the same for accurate testing [29]. Saouma et al. [29] proved that the fracture energy of the concrete was inversely proportional to the fracture process zone, which could be reduced to its half value by scaling down the aggregate size [28,29].

Four different materials were utilized to investigate the effect of the new geopolymer. To this end, i. Conventional concrete (C Specimens), ii. New geopolymer concrete (NGC Specimens), ii. Conventional concrete with recycled aggregate (C-R Specimens) and iv. New geopolymer concrete with recycled aggregate (NGC-R Specimens) were prepared. The shear behavior of specimens was investigated by performing four-point bending experiments with a displacement-controlled loading protocol. For that purpose, beam specimens have dimensions as 150 × 250 × 1100 mm, were designed with deficient lateral reinforcement detailing (i.e., spacing two times the code-required spacing). This choice is mainly to investigate shear – dominated behavior of this new construction material. The details on the reinforcements are given in Fig. 4.

Investigation of the mechanical properties as the compressive and splitting tensile strength of the material was carried out by tests conducted on the standard cylinder specimens (i.e., 150 × 300 mm), related results were presented in Table 4. Besides, for each

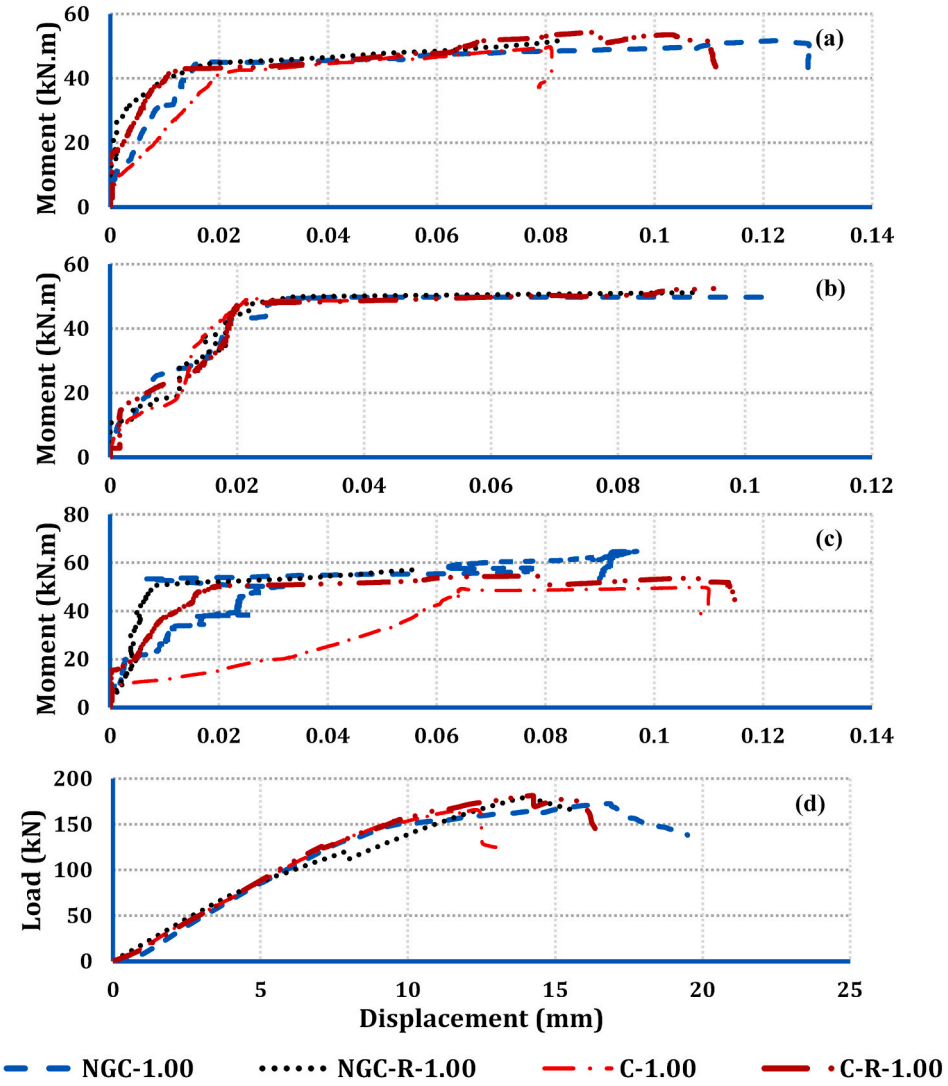

Fig. 8. M − ϕ Relationship for a/d = 1.00: (a) M-ϕ curve of left LVDTs, (b) M-ϕ curve of mid-LVDTs, (c) M-ϕ curve of right LVDTs, and (d) Total vertical load-midspan vertical displacement.

specimen the standard deviations of all results were noted in parenthesis. It should be noted that the deviations in the mechanical properties were slightly larger in new geopolymer concrete. In addition, the utilization of recycled aggregate had an adverse impact in terms of the flexural tensile strength (i.e., nearly 10% flexural tensile strength loss for both C and NGC specimens). The yield strength and ultimate strength for the specimens have 10-mm (6.5-mm) bars were detected as 456 MPa (330 MPa) and 716 MPa (449 MPa), respectively. Tie spacing was selected as 200 mm and taken as constant throughout the beam. 135° hooks were anchored to secure all of the ties to the core.

During each test, two-point vertical loads were applied on simply supported beam specimens with the help of the hydraulic actuator. In the tests, the applied vertical force values were recorded and the vertical deflection was monitored with Linear Variable Differential Transformers (LVDTs) inserted at the center of specimen. In addition, the mean curvature responses of all test beams were also detected by utilizing lateral LVDTs. At 50-mm intervals, lateral LVDTs were put on beam specimens. The details of the test setup are presented in Fig. 5. To evaluate the performance of new geopolymer concrete, load-deflection curves, moment-curvature (M-ϕ) curves, and pattern of crack propagation were utilized.

4. Test results

The test results are summarized in this section. The results are presented by classifying them with respect to their observed failure modes. Therefore, firstly, the test results of beam specimens with a shear span-to- effective depth ratio (a/d) of 0.50 were reported by documenting the observed pattern of crack, the load-deflection curves, and the M-ϕ curves. The curvature values were determined using the recordings of the lateral LVDTs placed at the top and bottom of the beam specimens over a known gage length (Fig. 5). Firstly,

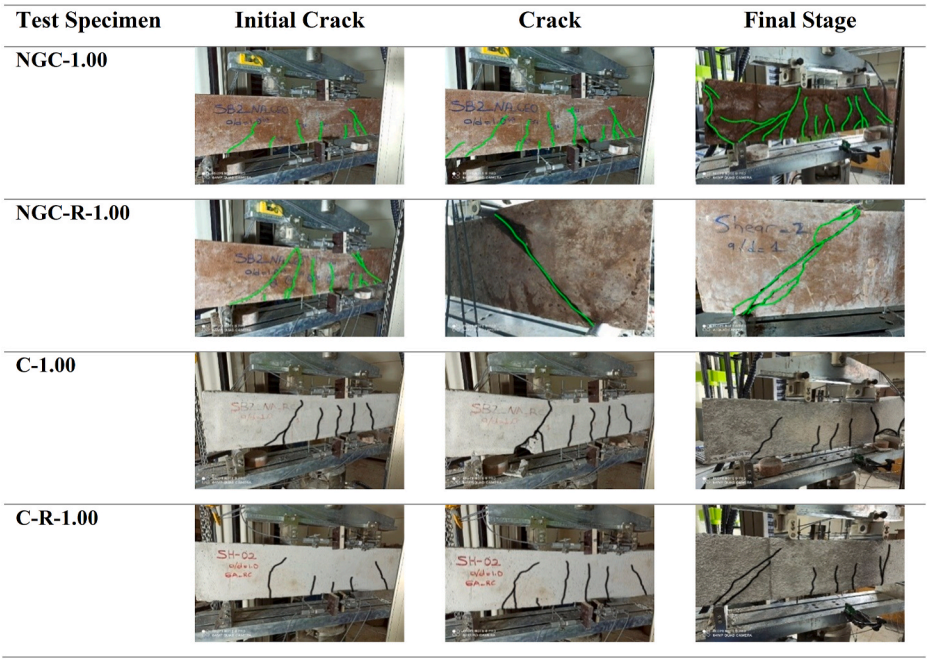

Fig. 9. Pattern of crack propagation of specimens (a/d = 1.00).

the average top and bottom strain were calculated from the recordings of the top and bottom horizontal LVDTs. Then, the curvature was determined by calculating the ratio of absolute top and bottom strains to the vertical distance between the lateral LVDTs. Then, other groups with different a/d ratios are given. Test results were summarized in terms of test result parameters. The explanation of test result parameters can be found in Table 5.

4.1. Beam specimens test results for a/d = 0.50

Total vertical load-deflection as well as M-ϕ characteristic of C-0.50, C-R-0.50, NGC-0.50, NGC-R-0.50 are shown in Fig. 6. Performance characteristics at the yield and ultimate loads and their corresponding displacements are presented in Table 6. Brittle response was observed for all geopolymer beam specimens without any exceptions. Besides, the post-yield response was not recorded even to a limited extent. Such finding was further corroborated by the observed pattern of crack (Fig. 7).

All specimens tested with an a/d ratio of 0.50 failed in shear, independent from the construction material behaved in a brittle way, implied by their load-deflection & M-ϕ curves. The failure of each specimen resulted from a large inclined crack in the shear span (Fig. 7). Thus, the M-ϕ curves showed a limited deviation from the linear range. It could easily be stated from Fig. 6 that the load/deflection capacities were similar for all construction materials. If the normalized energies are compared, it could be claimed that the inclusion of recycled aggregate brings about a decrement in the capacity of energy dissipation. In summary, if the shear-dominant behavior of reinforced geopolymer concrete was researched, geopolymer concrete could perform almost the same as the conventional reinforced concrete. Furthermore, all specimens' displacement and curvature ductilities were found to be extremely low (Table 6). Similar findings were observed in the literature that the strut mechanism was more dominant than the effect of matrix properties and type of aggregate in the shear resistance contribution at lower a/d ratios [30].

4.2. Beam specimen test results for a/d = 1.00

As a result of the experiments, the responses of vertical load-deflection and M-ϕ were presented in Fig. 8 for the C-1.00, C-R-1.00, NGC-1.00 and NGC-R-1.00 specimens. The yield and ultimate loads and their corresponding displacements, additionally the ductilities of specimens, were also given in Table 6. The brittle behavior of all specimens can be conveniently seen in Fig. 8. The post-yielded response was not observed, even with a limited degree, as also confirmed with pattern of crack propagation (Fig. 9). Besides, it was evident that specimens failed due to a shear cracking that reached to support (Fig. 9).

All specimens failed in shear-dominated action, as specimens with a/d = 0.5, displaying themselves as inclined cracks located in the region between the support and loading point. However, these specimens showed slightly more curvature ductilities, inferred by the yield plateau in M-ϕ curves (Fig. 8). It is significant to note that the right LVDTs placed on specimens C-1.00 had some problem at the initial stage, but they started recording after some time. Each specimen's curvature ductility values were quite near to 5. The failure patterns of each test specimen were observed to be equivalent (Fig. 9). The impact of recycled aggregate addition was seen to be negligible for these test specimens. It could be concluded that the usage of recycled aggregate on geopolymer concrete performance has limited impact, as performances of reinforced geopolymer concrete and conventional concrete were comparable level. Besides, the normalized energy dissipation capacity of the NGC specimen was significantly larger than others, but the remaining values were close

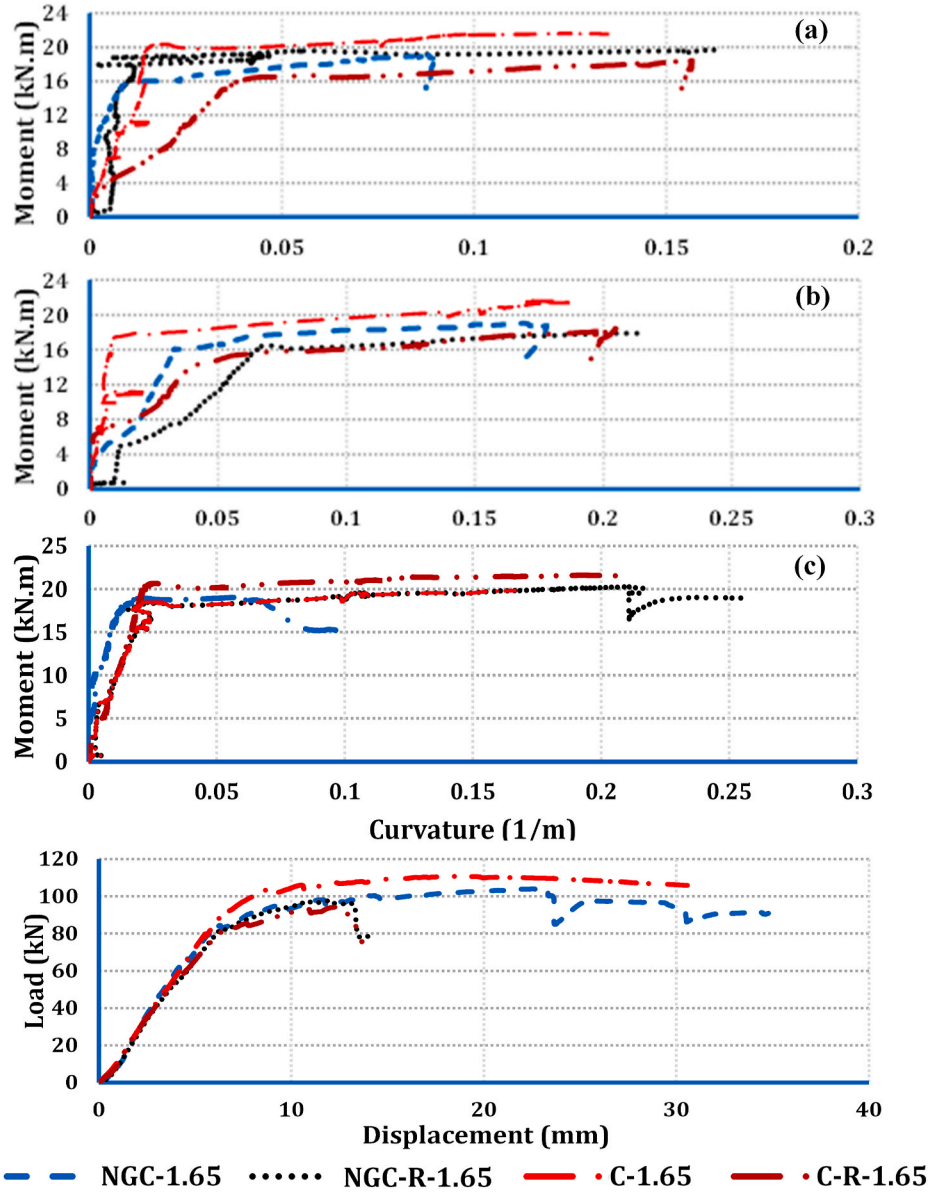

Fig. 10. M − ϕ Relationship for a/d = 1.65: (a) the M − ϕ curve of left LVDTs, (b) the M − ϕcurve of mid-LVDTs, (c) the M − ϕcurve of right LVDTs, and (d) Total vertical load-midspan vertical displacement.

to each other (Table 6).

4.3. Beam specimen test results for a/d = 1.65

The a/d ratio of 1.65 was chosen to examine the potential shear-flexure failure (Figs. 10 and 11). Load-deflection and M-ϕ responses of C-1.65, C-R-1.65, NGC-1.65, and NGC-R-1.65 are presented in Fig. 10. The yield & ultimate loads and corresponding displacements, as well as ductilities, are summarized in Table 6. As expected, all specimens failed due to mixed shear and flexure cracks observed in the shear span and constant moment span, respectively. However, it should be noted that specimens lost their capacity due to the enlargement of inclined cracks. For this type of failure, the effect of recycled aggregates was significant. The inclusion of recycled aggregate resulted in a considerable reduction in the displacement ductility. However, the curvature ductility was not significantly affected by the recycled aggregates. Specimens without recycled aggregate showed an extensive yield plateau. However, specimens with recycled aggregates showed analogical behaviour to the specimens with a/d = 1.00. E_n of specimens without recycled aggregate were nearly two times their counterparts. Therefore, geopolymer concrete and conventional concrete are approximately alike in the absence of recycled aggregates.

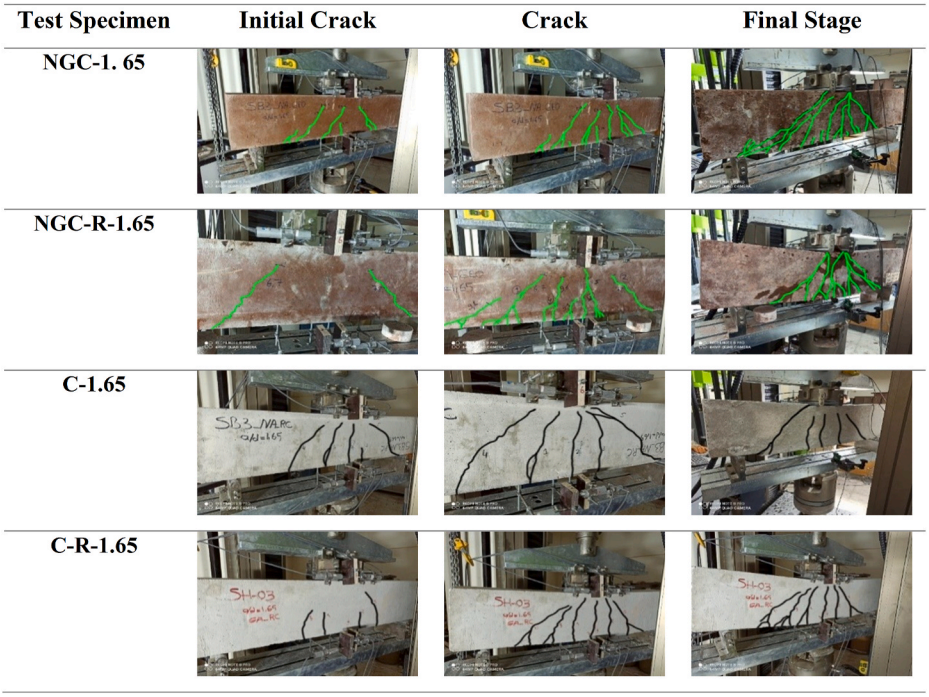

Fig. 11. Pattern of crack propagation of specimens (a/d = 1.65).

5. Discussion of test results

The compressive strength test results revealed that the C and NGC test specimens containing NAG have compressive strengths similar to one another considering their standard deviations. In parallel with the past studies in the literature [31,32], it was note that the compressive strength of NGC specimens containing NAG was higher than those containing RAG. On the contrary, there is approximately 3% increase in the compressive strength in the C-R mix compared to C specimens. According to previous studies, utilizing RAG in the mixture causes reduction in compressive strength and workability while leading an increase in the water absorption rate of both geopolymer and concrete mixtures [32,33] due to porous and rough surface texture of RAG particles [32,34,35]. However, it has been observed that the use of RAG, which has a very high-water absorption capacity, reduces the w/c ratio of the mixture. The slight increase in compressive strength in concrete specimens containing RAG can be attributed to the decrease in w/c ratio due to above-mentioned reasons. By contrast to the compressive strength, splitting tensile strength values showed that all mixes containing RAG were relatively weaker in strength than those prepared with NAG. This could be explained by the fact that the RAG failed through the aggregate in addition to the former ITZ, different than natural aggregates [49]. In the mixtures containing RAG, the effect of the ITZ surface could be observed more easily on the splitting tensile strength due to fissure effect applying on the specimen. In addition to this, RAG tends to deform quicker than NAG as it has lower modulus of elasticity, implied by the lower initial stiffness in specimens with RAG independent from the a/d ratio (Table 6). This observation was also mentioned in other studies [32,34,35].

The test results of shear-critical beams revealed that the behavior of the GPC specimens was similar to the CC specimens for all selected a/d ratios. In addition, except for specimens with an a/d ratio of 1.65, a large crack among the support and load application point was observed, causing the failure of specimens. Besides, the observed shear cracks in those specimens were detected to be formed through the aggregates proving that the geopolymer paste was more robust than the used natural and RAGs (Figs. 12–13). Similar observations related to the shear crack mechanism existed for conventional concrete specimens. More importantly, the failure mechanism was insensitive to the inclusion of RAGs for a/d ratios less than 1.65 (i.e., shear-dominated regions). This was mainly because the shear resistance was not entirely dependent on the tensile strength of the concrete. The shear strength was a combination of different resistant mechanisms: Dowel action of the longitudinal reinforcement, uncrushed concrete in compression side, capacity of ties, aggregate interlock, and the tensile strength of concrete. Huber et al. [35] was also claimed that dowel action of the longitudinal reinforcement, uncrushed concrete in compression side and aggregate interlock dominate the shear behavior of unreinforced concrete specimens. Therefore, the impact of RAG was more pronounced in the flexure capacity.

On the contrary, the beam specimens with an a/d ratio of 1.65 showed different performances depending on the using of RAG. The inclusion of the RAG caused a shift in the shear-dominated behavior, implied by the reduced ductility and normalized dissipated energies. The main responsible for this behavior may be the formation of the interfacial transition zone (ITZ) resulted from the use of RAG, considering the fact that the ductility of beams under flexural is directly affected by the bond strength of matrix and aggregate phase [36]. However, the test results showed that failure mode is highly dependent on the failure mode (i.e., a/d ratio). Due to the former attached mortar material around the RAGs, an ITZ development was seen in combination with RAGs, which is the most critical

Fig. 12. Close look-up to the final state of shear cracks of test specimens with an a/d ratio of 0.50.

element impacting this bond strength. Less amount of ductility in the shear-flexure failure could be attributed to the weakness of the extra ITZ formed in the mixtures in the presence of RAGs. This ITZ formation adversely affected the flexural capacity, delayed the occurrence of shear cracks. This statement was supported with a comparison of the flexural performances of beams with or without produced with RAGs (Table 4). Table 3 revealed that the flexural performances of beams containing RAGs reduced by approximately 10%.

In addition, the available capacity prediction equations are examined in this part. Accordingly, the experimental shear capacity of each specimen (V_{max}) was calculated by taking the minimum of the recorded maximum shear force (F_{max}) and the ratio of the recorded maximum moment and the shear span (i.e., M_{max}/a). Besides, the nominal moment capacity (M_n) and the nominal shear capacity (V_n) were calculated by the equations given in ACI 318-19 [37] and TS500 [38], respectively. The predicted nominal capacity (V_{cap}) was taken as the minimum of the nominal shear capacity (V_n) and the ratio of the nominal moment capacity and the shear span (i.e., M_n/a). These calculated values are presented in Table 7. It could be concluded that the estimation performance of both codes is very similar to each other, although the prediction of TS500 equations is slightly better. The absolute minimum percentage errors of ACI318-19 (TS500) equations for different a/d ratios are 61.68% (59.61%), 67.44% (65.77%) and 35.44% (33.04%), respectively. This result could be attributed to the mode of failure observed in the tested specimens. It is apparent that all the tested specimens had an a/d ratio less than 2 whereas the equation in ACI318-19 was proposed based on test results of specimens with an a/d ratio larger than 2. Therefore, the strut action was prevailing in the current study contrary to controlling diagonal tension failure in the code formulations. In addition, it should be noted that the code predictions resulted in over-conservative capacities for all specimens.

6. Conclusions

In this study, four different materials were utilized to investigate the effect of the new geopolymer and the inclusion of the recycled aggregate on the behavior. To this end, i. Conventional concrete (C Specimens), ii. New geopolymer concrete (NGC Specimens), ii.

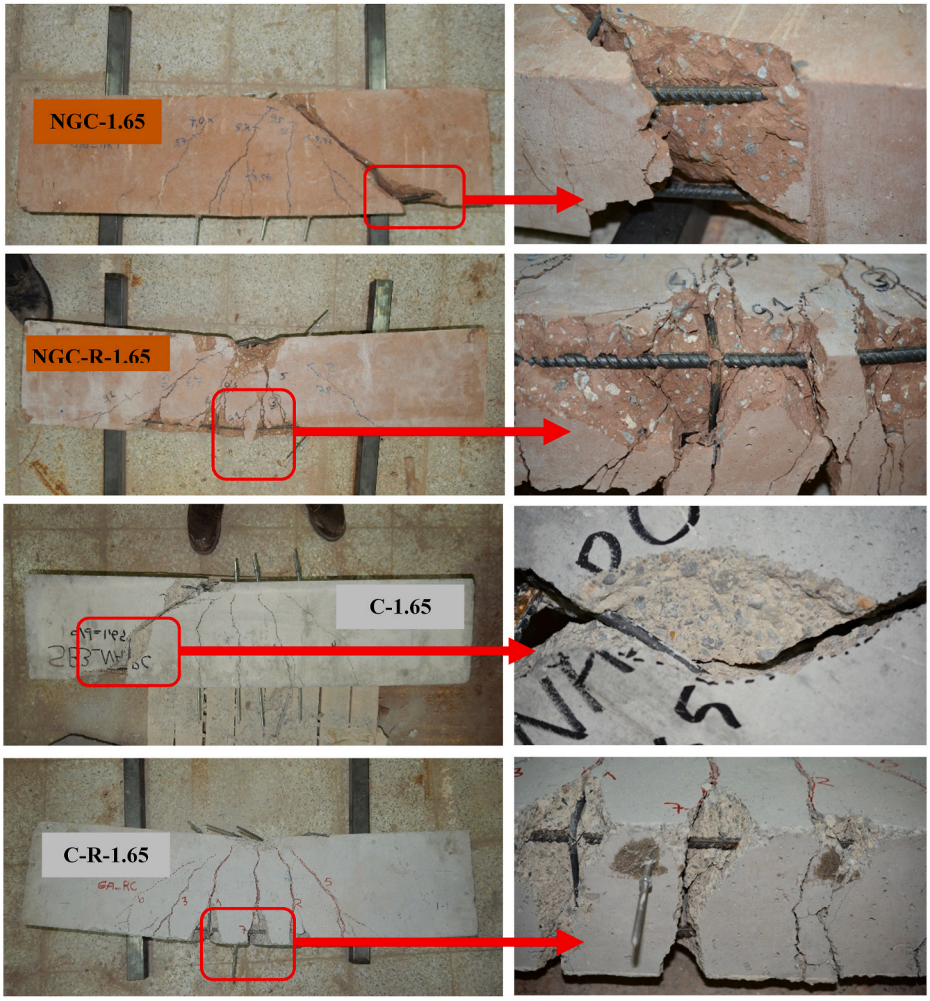

Fig. 13. Close look-up to the final state of shear cracks of test specimens with an a/d ratio of 1.65.

Table 7
Prediction performance of code equations.

Test Specimen	a/d	Experiment			TS500				ACI318-19			
		M_{max} (kN.m)	F_{max} (kN)	V_{max} (kN)	M_n (kN.m)	V_n (kN)	V_{cap} (kN)	Error (%)	M_n (kN.m)	V_n (kN)	V_{cap} (kN)	Error (%)
C	0.50	11.71	195.24	97.58	15.01	63.99	32.00	−67.21	12.76	60.73	30.36	−68.88
C-R	0.50	9.6	159.94	79.97	15.10	64.61	32.30	−59.61	12.89	61.29	30.64	−61.68
NGC	0.50	9.85	164.18	82.08	15.16	65.86	32.93	−59.88	12.98	62.43	31.21	−61.97
NGC-R	0.50	12.38	206.32	103.16	15.08	65.37	32.69	−68.32	12.91	61.99	30.99	−69.96
C	1.00	23.75	190.03	95.00	15.01	63.99	32.00	−66.32	12.76	60.73	30.36	−68.04
C-R	1.00	23.94	191.49	95.75	15.10	64.61	32.30	−66.26	12.89	61.29	30.64	−67.99
NGC	1.00	24.05	192.4	96.20	15.16	65.86	32.93	−65.77	12.98	62.43	31.21	−67.55
NGC-R	1.00	23.8	190.4	95.20	15.08	65.37	32.69	−65.67	12.91	61.99	30.99	−67.44
C	1.65	21.61	110.82	55.41	15.01	63.99	32.00	−42.25	12.76	60.73	30.36	−45.20
C-R	1.65	18.51	94.93	47.46	15.10	64.61	32.30	−31.94	12.89	61.29	30.64	−35.44
NGC	1.65	20.26	103.89	51.95	15.16	65.86	32.93	−36.61	12.98	62.43	31.21	−39.91
NGC-R	1.65	19.04	97.63	48.82	15.08	65.37	32.69	−33.04	12.91	61.99	30.99	−36.51

Conventional concrete with recycled aggregate (C-R Specimens) and iv. New geopolymer concrete with recycled aggregate (NGC-R Specimens) were prepared. For each material type, the flexural behavior was appointed by carrying out a four-point bending test with displacement-controlled loading methodology and three shear-span-to-depth ratios. Basis of the data from the tests performed in this study, the following key conclusions can be drawn:

1 All specimens with a/d ratios of 0.50 and 1.00 failed in shear, independent from the construction material, implied by brittle load-deflection and M-ϕ responses. The failure of each specimen resulted from a large inclined crack in the shear span (Figs. 6 and 8).
2 Specimens with an a/d ratio of 1.65 showed a combined shear-flexure failure, depending on the use of recycled aggregate. For this type of failure, the effect of recycled aggregates was significant. Specimens with recycled aggregates showed a smaller yield plateau in load-deflection curves due to the shift in the failure mode from the flexure-dominant to shear-dominant. En of specimens without RAGs were nearly two times their counterparts.
3 The failure mechanism was insensitive to the inclusion of recycled aggregates for a/d ratios less than 1.65 (i.e., shear-dominated regions). This was mainly because the shear resisting mechanism of reinforced concrete specimens was not completely interconnected to the tensile strength of concrete. The shear strength was a combination of different resistant mechanisms: Dowel action of the longitudinal reinforcement, uncrushed concrete in compression side, capacity of ties, aggregate interlock, and the tensile strength of concrete. Therefore, the impact of RAG was more apparent in the flexure capacity.
4 The ultimate moment capacity prediction performance of current codes is very similar to each other, although the prediction of TS500 equations is slightly better. The absolute minimum percentage errors of ACI318-19 (TS500) equations for different a/d ratios are 61.68% (59.61%), 67.44% (65.77%) and 35.44% (33.04%), respectively.

Credit author statement

Alper Aldemir: Conceptualization, Methodology, Writing, **Şaban Akduman:** Testing, **Oznur Kocaer:** Writing, **Rafet Aktepe:** Testing, **Mustafa Şahmaran:** Funding acquisition, Project administration, Editing, **Gürkan Yıldırım:** Review, **Hanady Almahmood:** Review, **Ashraf Ashour:** Funding acquisition, Review.

Declaration of competing interest

The authors declare no conflict of interest.

Acknowledgments

The authors gratefully acknowledge the financial assistance of the Scientific and Technical Research Council (TUBITAK) of Turkey and the British Council provided under projects: 218M102 and European Union's Horizon 2020 research and innovation programme under grant agreement No: 869336, ICEBERG (Innovative Circular Economy Based solutions demonstrating the Efficient recovery of valuable material Resources from the Generation of representative End-of-Life building material). This work was also supported by Newton Prize 2020.

References

[1] J. De Brito, N. Saikia, Recycled Aggregate in Concrete: Use of Industrial, Construction and Demolition Waste, Springer Science & Business Media, 2012.
[2] S. Luhar, S. Chaudhary, I. Luhar, Development of rubberized geopolymer concrete: strength and durability studies, Construct. Build. Mater. 204 (2019) 740–753, https://doi.org/10.1016/j.conbuild mat.2019.01.185.
[3] G. Yildirim, A. A Kul, E. Özçelikci, M. Sahmaran, A. Aldemir, D. Figueira, A.F. Ashour, Development of alkali-activated binders froRecycled mixed masonry-originated waste, J. Build. Eng. 33 (2020) 101690.
[4] H. Ulugöl, A. Kul, G. Yıldırım, M. Şahmaran, A. Aldemir, D. Figueira, A.F. Ashour, Mechanical and microstructural characterization of geopolymers from assorted construction and demolition waste-based masonry and glass, J. Clean. Prod. 280 (1) (2020) 1–15, https://doi.org/10.1016/j.jclepro.2020.124358.
[5] D. McKelvey, V. Sivakumar, A. Bell, G. McLaverty, Shear strength of recycled construction materials intended for use in vibro ground improvement, Ground Improv. 6 (2) (2002) 59–68.
[6] X.Y. Zhuang, L. Chen, S. Komarneni, C.H. Zhou, D.S. Tong, H.M. Yang, H. Wang, Fly ash-based geopolymer: clean production, properties and applications, J. Clean. Prod. 125 (2016) 253–267.
[7] J. Davidovits, V. Mohan, High –alkali cements for 21st century concretes in concrete technology, past, present and future, in: Malotra Symposium, vol. 144, ACIP, 1994, pp. 383–397.
[8] F. Pelısser, B.V. Sılva, M.H. Menger, B.J. Frasson, T.A. Keller, A.J. Torıı, R.H. Lopez, Structural Analysis of Composite Metakaolin-Based Geopolymer Concrete, vol. 11, June 2018, pp. 535–543. ISSN 1983-4195.
[9] A.L. Mohammed Al-Majidi, Andrew cundy, effect of alkaline activator, water, superplasticiser and slag contents on the compressive strength and workability of slag-fly ash based geopolymer mortar cured under ambient temperature, World Academy of Science, Engineering and Technology International Journal of Civil, Environmental, Structural, Construction and Architectural Engineering 10 (3) (2016).
[10] S.D. Raj, N. Ganesan, R. Abraham, A. Raju, Behavior of geopolymer and conventional concrete beam column joints under reverse cyclic loading, Advances in Concrete Construction 4 (No. 3) (2016) 161–172.
[11] H.Q. Ahmet, D.K. Jaf, Ş.A. Yaseen, Flexural capacity and behaviour of geopolymer concrete beams reinforced with glass fibre-reinforced polymer bars, International Journal of Concrete Structures and Materials 14 (No. 1) (2020).
[12] C. Wu, H. Hwang, C. Shi, N. Li, Y. Du, Shear tests on reinforced slag-based geopolymer concrete beams with transverse reinforcement, Eng. Struct. 219 (15 September 2020) 110966.
[13] D.M.J. Sumajouw, D. Hardjito, S.E. Wallah, B.V. Rangan, Fly ash-based geopolymer concrete: study of slender reinforced columns Journal of Materials Science May 2007, International Journal of Concrete Structures and Materials (2020).
[14] T.T. Tran, T.M. Pham, H. Hao, Effect of hybrid fibers on shear behaviour of geopolymer concrete beams reinforced by basalt fiber reinforced polymer (BFRP) bars without stirrups, Compos. Struct. 243 (1) (2020).
[15] S. Akduman, O. Kocaer, A. Aldemir, M. Sahmaran, G. Yıldırım, H. Almahmood, A. Ashour, Experimental investigations on the structural behaviour of reinforced geopolymer beams produced from recycled construction materials, J. Build. Eng. 41 (1) (2021) 1–12.
[16] T.T. Tran, T.M. Pham, H. Hao, Experimental and analytical investigation on flexural behaviour of ambient cured geopolymer concrete beams reinforced with steel fibers, Eng. Struct. 200 (1) (2019).
[17] N.A. Farhan, M.N. Sheikh, M.N.S. Hadi, Behaviour of ambient cured steel fibre reinforced geopolymer concrete columns under axial and flexural loads, Structure 15 (1) (2018) 184–195.
[18] Turkish Earthquake Code (TEC2018), Specifications for the Buildings to Be Constructed in Disaster Areas, Prime Ministry Disaster and Emergency Management Authority, Ankara, Turkey, 2018.

[19] K. Komnitsas, D. Zaharaki, A. Vlachou, G. Bartzas, M. Galetakis, Effect of synthesis parameters on the quality of construction and demolition wastes (CDW) geopolymers, Adv. Powder Technol. 26 (2015) 368–376.
[20] S. Kumar, F. Kristály, G. Mucsi, Geopolymerisation behaviour of size fractioned fly ash, Adv. Powder Technol. 26 (2015) 24–30.
[21] T.E. Azak, B.O. Ay, S. Akkar, A statistical study on geometrical properties of Turkish reinforced concrete building stock, in: 2nd European Conference on Earthquake Engineering and Sesimology, Istanbul, Turkey, 2014.
[22] A. Aldemir, B. Binici, E. Canbay, A. Yakut, Lateral load testing of an existing two story masonry building up to near collapse, Bull. Earthq. Eng. 15 (8) (2017) 3365–3383.
[23] H. Sucuoglu, W. Lin, B. Binici, P. Ezzatfar, Pseudo-dynamic testing, performance assessment, and modeling of deficient reinforced concrete frames, ACI Struct. J. 111 (5) (2014) 1203–1212.
[24] T.K. Sipos, V. Sigmund, M. Hadzima-Nyarko, Earthquake performance of infilled frames using neural networks and experimental database, Eng. Struct. 51 (1) (2013) 113–127.
[25] A. Aldemir, B. Binici, E. Canbay, Cyclic testing of reinforced concrete double walls, ACI Struct. J. 114 (2) (2017) 395–406.
[26] Gharibdoust, A., Aldemir A. and Binici B. “Seismic behaviour of roller compacted concrete dams under different base treatments. Structure and Infrasturture Engineering 16(2). 355-366.
[27] Y. Uchita, T. Shimpo, V. Saouma, Dynamic centrifuge tests of concrete dam, Earthq. Eng. Struct. Dynam. 34 (12) (2005) 1467–1487.
[28] V. Saouma, J. Broz, E. Brühwiler, H. Boggs, Effect of aggregate and specimen size on fracture properties of dam concrete, J. Mater. Civ. Eng. 3 (3) (1991) 204–218.
[29] G. Fathifazl, A.G. Razaqpur, O.B. Isgor, A. Abbas, B. Fournier, S. Foo, Shear strength of reinforced recycled concrete beams without stirrups, Mag. Concr. Res. 61 (7) (2009) 477–490.
[30] K. Rahal, Mechanical properties of concrete with recycled coarse aggregate, Build. Environ. 42 (1) (2007) 407–415.
[31] M. Etxeberria, E. Vázquez, A. Marí, M. Barra, Influence of amount of recycled coarse aggregates and production process on properties of recycled aggregate concrete, Cement Concr. Res. 37 (5) (2007) 735–742.
[32] P. Nuaklong, A. Wongsa, V. Sata, K. Boonserm, J. Sanjayan, P. Chindaprasirt, Properties of high-calcium and low-calcium fly ash combination geopolymer mortar containing recycled aggregate, Heliyon 5 (9) (2019), e02513.
[33] M.C. Rao, S.K. Bhattacharyya, S.V. Barai, Influence of field recycled coarse aggregate on properties of concrete, Mater. Struct. 44 (1) (2011) 205–220.
[34] H.J. Chen, T. Yen, K.H. Chen, Use of building rubbles as recycled aggregates, Cement Concr. Res. 33 (1) (2003) 125–132.
[35] T. Huber, P. Huber, J. Kollegger, Influence of aggregate interlock on the shear resistance of reinforced concrete beams without stirrups, Eng. Struct. 186 (2019) 26–42.
[36] A. Akbarnezhad, K.C.G. Ong, M.H. Zhang, C.T. Tam, T.W.J. Foo, Microwave-assisted beneficiation of recycled concrete aggregates, Construct. Build. Mater. 25 (8) (2011) 3469–3479.
[37] American concrete institute (ACI), “building code requirements, structural concrete and commentary”, ACI Committee 318 (2011).
[38] Turkish Standards (TS500), Design and Construction Rules of Reinforced Concrete Structures, Turkish Standards Institute, Ankara, Turkey, 2000.